# Self-force in Hyperbolic Scattering: a Frequency Domain Approach

Chris Whittall
Supervisor: Leor Barack

23rd International Conference on GR and Gravitation
5th July 2022

# Scatter orbits as strong-field probe of GR

Scatter angle defined by

$$\delta\varphi := \varphi_{out} - \varphi_{in} - \pi$$
$$= \delta\varphi^{(0)} + \eta\delta\varphi^{(1)} + \eta^2\delta\varphi^{(2)} + \ldots \quad (1)$$

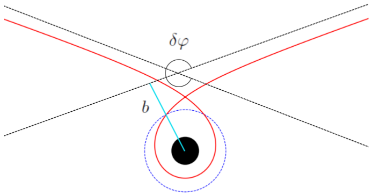


Motivations:

- Conservative PM dynamics can be inferred from self-force scatter calculations, valid at *all* mass ratios. [Damour 2020]
- Benchmarking PM results in the strong-field regime.
- Strong-field probe of GR potential.
- Comparisons with quantum amplitude methods.
- Calibrate effective-one-body models.
- Hence inform an accurate universal model of BBH inspirals, suitable for GW searches.

# Frequency domain

- FD codes exist to calculate first-order GSF along generic bound Kerr geodesics [Van de Meent 2017]. Several challenges when moving to unbound orbits.
- Despite this, we are interested in frequency-domain methods due to potentially higher precision and efficiency.
- We work with **scalar field toy model** in Schwarzschild to investigate problems and solutions:
  - Continuous spectra
  - UV problem near the particle
  - Slowly convergent radial integrals

# Field equation

The scalar field equation is given by

$$\nabla_\mu \nabla^\mu \Phi = -4\pi T \tag{2}$$

and the scalar charge density $T$ is that of a point particle. We separate into spherical and Fourier harmonics:

$$\Phi = \int d\omega \sum_{\ell,m} \frac{1}{r} \psi_{\ell m\omega} Y_{\ell m}(\theta,\varphi) e^{-i\omega t}, \tag{3}$$

and the equation of motion becomes

$$\frac{d^2\psi_{\ell m\omega}}{dr_*^2} - (V_\ell(r) - \omega^2)\psi_{\ell m\omega} = S_{\ell m\omega}(r). \tag{4}$$

# Inhomogeneous solution

For $\omega \neq 0$ variation of parameters gives us the inhomogeneous field

$$\begin{aligned}\psi_{\ell m\omega}(r) = \psi^{+}_{\ell m\omega}(r)\int_{r_{min}}^{r}\frac{\psi^{-}_{\ell m\omega}(r')S_{\ell m\omega}(r')}{W_{\ell m\omega}}\frac{dr'}{f(r')}\\ + \psi^{-}_{\ell m\omega}(r)\int_{r}^{\infty}\frac{\psi^{+}_{\ell m\omega}(r')S_{\ell m\omega}(r')}{W_{\ell m\omega}}\frac{dr'}{f(r')},\end{aligned} \tag{5}$$

where for $\omega \neq 0$ the homogeneous solutions $\psi^{\pm}_{\ell m\omega}$ are defined by BCs:

$$\psi^{-}_{\ell m\omega}(r) \sim e^{-i\omega r_*} \quad \text{as } r_* \longrightarrow -\infty \tag{6}$$

$$\psi^{+}_{\ell m\omega}(r) \sim e^{+i\omega r_*} \quad \text{as } r_* \longrightarrow +\infty. \tag{7}$$

# Extended homogeneous solutions

- Delta function source causes slow, non-uniform convergence of Fourier series/integral near the worldline (Gibbs phenomenon).

- MEHS: express time domain field $\Phi_{lm}(t,r)$ in terms of analytic functions on either side of the worldline.

$$r\Phi_{\ell m}(t,r) = \tilde{\psi}^{+}_{\ell m}(t,r)\Theta(r - r_p(t)) + \tilde{\psi}^{-}_{\ell m}(t,r)\Theta(r_p(t) - r). \tag{8}$$

[Barack, Ori, Sago 2008]

- For bound orbit,

$$\tilde{\psi}^{\pm}_{\ell m\omega}(r) := \psi^{\pm}_{\ell m\omega}(r)\int_{r_{min}}^{r_{max}} \frac{\psi^{\mp}_{\ell m\omega}(r')S_{\ell m\omega}(r')dr'}{W_{\ell m\omega}f(r')}. \tag{9}$$

# EHS: unbound case

- EHS method relies on the existence of vacuum regions $r \geq r_{max}$ and $r \leq r_{min}$ where the EHS and physical fields coincide.
- Agreement throughout the domain is deduced using an analyticity argument.
- For the unbound case, we no longer have the $r \geq r_{max}$ vacuum region. But we do still have the vacuum region $r \leq r_{min}$.
- Attempts to apply a (modified) form of EHS outside the orbit have not been successful so far.

We can only use EHS to reconstruct the field **inside** the orbit.

# Slowly converging radial integrals

$$C^{-}_{\ell m\omega} := \int_{r_{min}}^{+\infty} \frac{\psi^{+}_{\ell m\omega}(r)\cos[\omega t_p(r) - m\varphi_p(r)]}{r|u^r(r)|} dr. \qquad (10)$$

- Integrand singular at $r_{min}$. Split integration region and use integration variable $\chi$ near periapsis, $r$ at distance.
- The integrand behaves like oscillations$/r$ at large $r$. Hence we have to integrate out to great distance to get convergence.
- At higher frequencies, need to integrate over many wavecycles, at great cost. A single integral can take $> 30s$ if done naively.

# Truncating the integral: problems

- Truncating at such radii causes issues in the tail of the spectrum.
- Suppressing this requires $r_{max}$ to increase by orders of magnitude. Not feasible due to runtime cost.
- Need to increase decay rate, speed up integration, or approximate tail. All are possible.

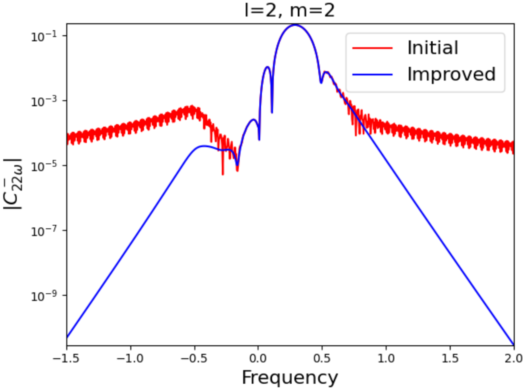


Figure: Red curve shows effect of truncating integral at $r_{max} = 1980M$. With new techniques, we obtain an improved spectrum

# Analytical approximations to the tail

The integrand of $C^{-}_{\ell m\omega}$,

$$J_{\ell m\omega}(r) := \frac{1}{2}\sum_{\sigma=\pm 1}\frac{\psi^{+}_{\ell l m\omega}(r')\exp\left[i\sigma\left(\omega t_p(r') - m\varphi_p(r')\right)\right]}{r'\left|u^r(r')\right|}, \tag{11}$$

has an expansion as $r \to \infty$. This series can be integrated to obtain an approximation to the neglected tail,

$$\int_{r_{max}}^{+\infty} J_{\ell m\omega}(r)dr \approx \frac{1}{2\sqrt{E^2-1}}\sum_{\sigma=\pm 1}\sum_{n=0}^{N}\lambda_\sigma^{(n)} e^{i\sigma\Delta_\infty^{(0)}} r_{max}^{a(n)} z^{-a(n)}\Gamma[a(n), z]. \tag{12}$$

This is very fast to evaluate. The limiting factor is deriving expressions for the $\lambda_\sigma^{(n)}$ in advance.

# Analytical approximations to the tail: impact

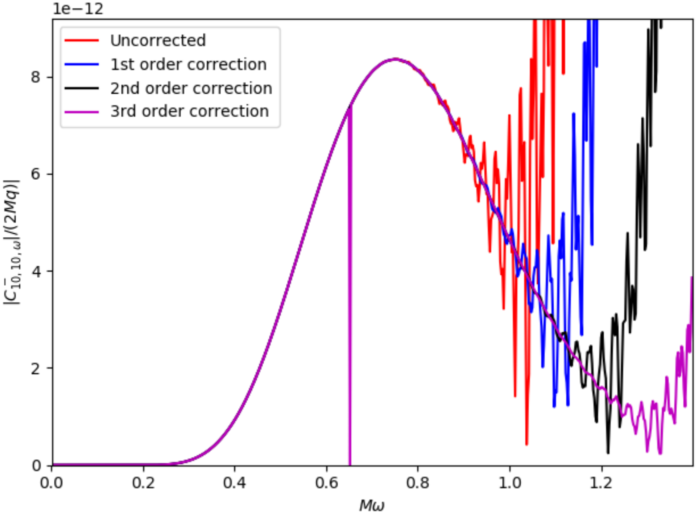


Have corrections up to 6th order, but this is not enough.

# Integration by parts (1)

Integration by parts can be used to increase the rate of convergence.

We can rewrite the integrand

$$J_{\ell m\omega}(r) := \frac{1}{2} \sum_{\sigma=\pm 1} e^{i\Omega_\sigma r} K^{\sigma}_{\ell m\omega}(r), \tag{13}$$

where $\Omega_\sigma := \omega(1 + \sigma/v)$ and the function $K^{\sigma}_{\ell m\omega}$ has the asymptotics

$$K^{\sigma}_{\ell m\omega} \sim r^{i\omega(1+\sigma B)-1} \tag{14}$$

as $r \to \infty$. Then we have the property

$$\frac{d^N K^{\sigma}_{\ell m\omega}}{dr^N} = O\left(\frac{1}{r^{N+1}}\right) \tag{15}$$

as $r \to \infty$.

# Integration by parts (2)

Applying integration by parts $N+1$ times,

$$C^{-(r)}_{\ell m\omega} = \frac{1}{2}\sum_{\sigma=\pm 1}\left\{\sum_{n=0}^{N}\left[\left(\frac{i}{\Omega_\sigma}\right)^{n+1} e^{i\Omega_\sigma r_{cut}} K^{\sigma(n)}_{\ell m\omega}(r_{cut})\right]\right.$$
$$\left. + \left(\frac{i}{\Omega_\sigma}\right)^{N+1}\int_{r_{cut}}^{+\infty} e^{i\Omega_\sigma r} K^{\sigma(N+1)}_{\ell m\omega}(r)dr\right\}. \quad (16)$$

Integration by parts can be applied as many times as required. Limited only by need to derive expressions for the derivatives $K^{\sigma(n)}_{\ell m\omega}$.

We have implemented 4 iterations of IBP, i.e. truncation error $O(r_{max}^{-5})$.

# Improved spectrum

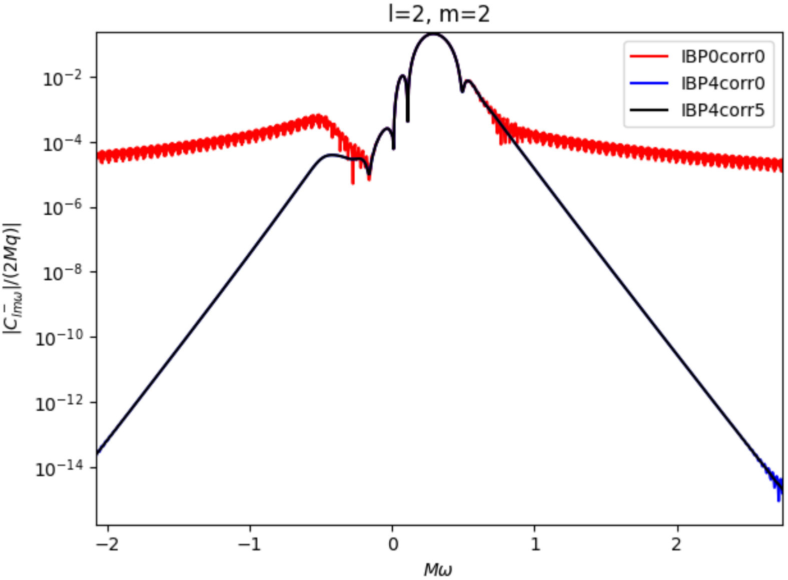

# Further efficiencies

- Clenshaw-Curtis quadrature suited to integrals with a sine/cosine weight function. Reduces runtime to 1-2$s$ for a single integral, increasing only slowly with $\omega$.
- Additionally, we can accurately interpolate $C^{-}_{\ell m\omega}$ over frequency, reducing number of integrals we need to evaluate.
- Calculation of integrals largely independent of each other $\implies$ highly parallelisable.

# Self-force calculation: $t$-component

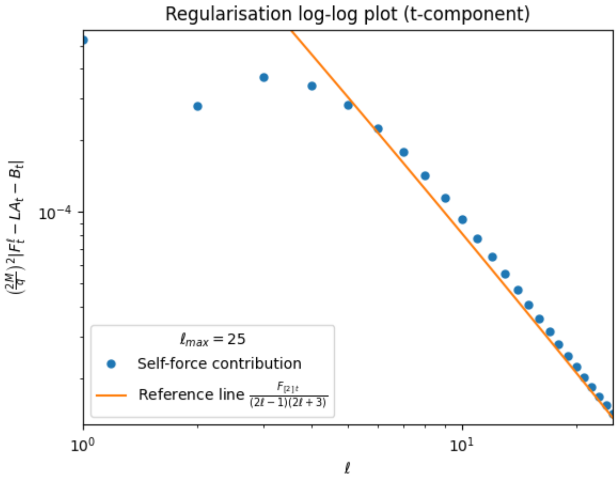


Calculation of the self-force passes regularisation tests

# Self-force calculation: other components

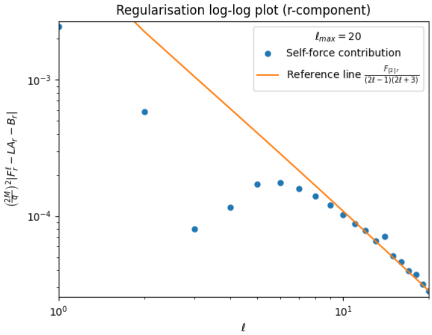


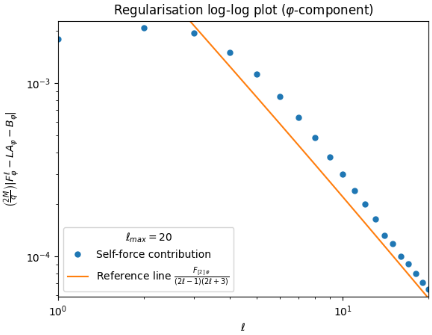


The other components also pass regularisation tests. These are more challenging to calculate due to low-frequency contributions.

# Summary and outlook

We have:

- Developed methods to improve the convergence and runtime of the integrals $C^-_{\ell m\omega}$.
- Demonstrated the ability to accurately interpolate $C^-_{\ell m\omega}$ over frequency.
- Obtained caculations of the self-force at selected points along the orbit.

Next steps:

- Resolve remaining issues with isolated modes.
- Scatter-angle calculation.
- Other observables e.g. time delay.
- Comparisons with PM results.